Critical temperature for shape transition in hot nuclei within covariant density functional theory

W. Zhang (张炜)[1,2] and Y. F. Niu (牛一斐)[3,*]

[1]*Henan Key Laboratory of Ion-beam Bioengineering, Zhengzhou University, Zhengzhou 450052, China*

[2]*Molecular Foundry, Lawrence Berkeley National Laboratory, Berkeley, California 94720, USA*

[3]*ELI-NP, Horia Hulubei National Institute for Physics and Nuclear Engineering, 30 Reactorului Street, RO-077125 Bucharest-Magurele, Romania*

(Received 28 December 2017; published 2 May 2018)

Prompted by the simple proportional relation between critical temperature for pairing transition and pairing gap at zero temperature, we investigate the relation between critical temperature for shape transition and ground-state deformation by taking even-even $^{286-304}$Cm isotopes as examples. The finite-temperature axially deformed covariant density functional theory with BCS pairing correlation is used. Since the Cm isotopes are the newly proposed nuclei with octupole correlations, we studied in detail the free energy surface, the Nilsson single-particle (s.p.) levels, and the components of s.p. levels near the Fermi level in ^{292}Cm. Through this study, the formation of octupole equilibrium is understood by the contribution coming from the octupole driving pairs with $\Omega[N,n_z,m_l]$ and $\Omega[N+1,n_z\pm 3,m_l]$ for single-particle levels near the Fermi surfaces as it provides a good manifestation of the octupole correlation. Furthermore, the systematics of deformations, pairing gaps, and the specific heat as functions of temperature for even-even $^{286-304}$Cm isotopes are discussed. Similar to the relation between the critical pairing transition temperature and the pairing gap at zero temperature $T_c = 0.6\Delta(0)$, a proportional relation between the critical shape transition temperature and the deformation at zero temperature $T_c = 6.6\beta(0)$ is found for both octupole shape transition and quadrupole shape transition for the isotopes considered.

DOI: 10.1103/PhysRevC.97.054302

I. INTRODUCTION

The study of hot nuclei has been a hot topic for decades. At medium excitation energies in heavy-ion fusion, a completely equilibrated system is formed before the compound nucleus decays by particle or γ emission [1]. The microcanonical description for the situation can be transformed to an approximate form in which the equilibrated nucleus is characterized by the temperature. When temperature rises, the shape deformations or superfluidity are expected to wash out. This can be understood in terms of the shell model [2]. By increasing temperature, nucleons are excited from levels below the Fermi surface to levels above, resulting in level blocking, and hence pairing correlations decrease. A similar picture holds for the shape transition. The increasing temperature leads to the repopulation of the single-particle levels near the Fermi surface, which will weaken the shell effects and hence act in the direction of decreasing the equilibrium deformation [2,3]. The equilibrium deformation can be extracted from experimental data such as giant dipole resonance (GDR). Extensive studies for the GDR built on excited states can be found in Refs. [4–8] and references therein. In the finite-temperature mean-field theory, these effects appear as sharp phase transitions including pairing transitions and shape transitions, although the sharp phase transitions will be actually washed out due to statistical fluctuations since the nucleus is a finite system. The statistical fluctuations can be treated in the spirit of the Landau theory [3,9] or from a more fundamental point of view by using path integral techniques such as the static path approximation [10,11], the shell-model Monte Carlo method [12], the particle number projected BCS method [13–15], or the shell-model-like approach [16].

However, finite-temperature mean-field models still provide a simple and good tool for the study of hot nuclei. Simple relations between the critical temperature for pairing transition T_c and pairing gap at zero temperature $\Delta(0)$ can be found in such models. For example, the critical pairing temperature is calculated to be $T_c = 0.57\Delta(0)$ in the finite-temperature BCS theory with a constant pairing force [17], $T_c = 0.5\Delta(0)$ using a simplified degenerate model [18], and $T_c = 0.6\Delta(0)$ in the finite-temperature relativistic Hartree-Bogoliubov theory [19]. Such a simple relation gives us a good guideline on up to which temperature the pairing correlations are important, which is instructive information for the study of hot nuclei and corresponding subjects, like weak interaction processes of nuclei in stellar environments [20], heavy-ion collisions [21,22], and so on.

Similarly, it would be also useful if the critical temperature for shape phase transition also holds a simple relation with the ground-state deformation, since above the critical temperature the deformation will vanish, and therefore nuclei could be studied as a spherical system, which simplifies the calculation a lot. The previous phenomenological studies give us some clues about it [3,23,24]. In Ref. [3], the general framework of the Landau theory was used to establish the free energy and entropy

*nyfster@gmail.com

dependence on the deformation and the temperature variables. In this work, the analytical expression for the equilibrium deformation as a function of temperature was obtained. As a further study, the systematics of the critical temperature and the critical angular momentum of the shape transitions as functions of neutron and proton number were investigated with Landau theory in Ref. [24]. It was found that the systematics of critical temperature is simple. The critical temperature as a function of the neutron number falls on an inverted parabola-like curve whose maximum is at the mid shell and minima near two closed neutron shells. The same behavior was also found as a function of proton number. It is obvious that such behavior is very similar to the behavior of the ground-state deformation. However, the possible relation between the critical temperature and the ground-state deformation was not pointed out.

In recent years, microscopic models for the study of shape transitions in hot nuclei were developed. The finite-temperature Hartree-Fock-Bogoliubov theory was formulated [18] and then applied to the pairing and shape transitions in rare-earth nuclei [25]. The shape transition from prolate to spherical occurs at 1.81 MeV for ^{170}Er, while ^{188}Os experienced two shape transitions, namely, one from a triaxial shape to an oblate shape at 0.60 MeV and the other from an oblate shape to spherical at 1.33 MeV. Using the finite-range density-dependent Gogny force and a large configuration space within the framework of the finite-temperature Hartree-Fock-Bogoliubov (FTHFB) theory [2], nuclei with different shapes, including well-quadrupole-deformed nuclei, superdeformed nuclei, and octupole-deformed nuclei, gradually collapse to the spherical shape at certain critical temperatures in the range 1.3–2.7 MeV.

The covariant density functional theory (CDFT), which has achieved great success in describing ground-state properties of both spherical and deformed nuclei all over the nuclear chart [26–32], is a good tool for investigations on nuclear properties with temperature. The finite-temperature relativistic Hartree-Bogoliubov theory [19] and relativistic Hartree-Fock-Bogoliubov theory [33] for spherical nuclei were formulated and used to study the pairing transitions in hot nuclei. The relativistic Hartree-BCS theory was applied to study the temperature dependence of shapes and pairing gaps for ^{166,170}Er and rare-earth nuclei [34,35]. A shape transition from prolate to spherical shapes was found at temperatures in the range 1.0–2.7 MeV. Taking into account the unbound nucleon states, the temperature dependence of the pairing gaps, nuclear deformation, radii, binding energies, and entropy were studied in the Dirac-Hartree-Bogoliubov (DHB) calculations [36,37]. It was also found that the nuclear deformation disappears at temperatures $T = 2.0-4.0$ MeV. When the temperature $T \geqslant 4$ MeV, the effects of the vapor phase that take into account the unbound nucleon states become important. Recently, the finite-temperature covariant density functional theory in the axially deformed space was developed and used to study the shape evolution of ^{72,74}Kr [38]. The shape transition temperature was found between 1.7 and 2.1 MeV. Furthermore, the octupole correlations were taken into account and the shape evolutions of typical octupole-deformed nuclei ^{224}Ra and even-even $^{144-154}$Ba isotopes were studied, and these nuclei first go through an octupole shape transition where the octupole correlations disappear at temperature range 0.5–0.95 MeV, and then another quadrupole shape transition from quadrupole-deformed shape to spherical shape at a higher temperature range 1.0–2.2 MeV [39]. Moreover, it was pointed out that the transition temperatures are roughly proportional to the corresponding deformations at the ground states.

Motivated by this study, we would like to investigate more carefully the possible relation between ground-state deformation and the critical temperature. To generalize our study, we take examples of nuclei with both octupole and quadrupole deformations. Traditionally, strong octupole correlations occur at the nucleon numbers being close to 56 ($1h_{11/2} \leftrightarrow 2d_{5/2}$ coupling), 88 ($1i_{13/2} \leftrightarrow 2f_{7/2}$ coupling), and 134 ($1j_{15/2} \leftrightarrow 2g_{9/2}$ coupling) [40]. For example, in the previous study of Ref. [39], ^{224}Ra with neutron number 136 and proton number 88, and even-even $^{144-154}$Ba isotopes with neutron number 88-98 and proton number 56 were selected as regions with possible octupole correlations. Recently, a new region centering at ^{292}Cm with neutron number 196 and proton number 96 were systematically studied and the ground-state octupole deformation was obtained by covariant density functional theory [41]. It is proposed that the neutron $1k_{17/2} \leftrightarrow 2h_{11/2}$ coupling and the proton $1i_{13/2} \leftrightarrow 2f_{7/2}$ coupling are responsible for the ground-state octupole deformation. The research concerning ^{292}Cm will shed light on the understanding of nuclear shape, especially octupole correlations and their related problems.

Therefore, the purpose of this paper is twofold. The first one is to study the relation between critical shape transition temperature and ground-state deformation by taking Cm isotopes as examples, and the other one is to explore in detail the newly suggested octupole nucleus ^{292}Cm by understanding how the octupole correlations manifest. So in this paper, the shape transition temperature together with the ground-state deformation is investigated for the even-even $^{286-304}$Cm isotopes in the CDFT framework. It is organized as follows. The self-consistent finite-temperature CDFT model with BCS approach for axially deformed nuclei based on the point-coupling density functional is briefly introduced in Sec. II. In Sec. III, the shape evolution of ^{292}Cm with temperature is studied in detail using the single-particle levels near the Fermi surfaces concerning the octupole correlations. Furthermore, the systematics of deformations, pairing gaps of the global minimum, and the specific heat as functions of temperature for even-even $^{286-304}$Cm isotopes are discussed. A proportional relation between ground-state deformation and critical temperature is explored.

II. THEORETICAL FRAMEWORK

The starting point of the CDFT model is an effective Lagrangian density with zero-range point-coupling interaction between nucleons:

$$\begin{aligned}\mathcal{L} = {} & \bar{\psi}(i\gamma_\mu\partial^\mu - m)\psi - \frac{1}{2}\alpha_S(\bar{\psi}\psi)(\bar{\psi}\psi) \\ & - \frac{1}{2}\alpha_V(\bar{\psi}\gamma_\mu\psi)(\bar{\psi}\gamma^\mu\psi) - \frac{1}{2}\alpha_{TV}(\bar{\psi}\vec{\tau}\gamma_\mu\psi)\cdot(\bar{\psi}\vec{\tau}\gamma^\mu\psi) \\ & - \frac{1}{3}\beta_S(\bar{\psi}\psi)^3 - \frac{1}{4}\gamma_S(\bar{\psi}\psi)^4 - \frac{1}{4}\gamma_V[(\bar{\psi}\gamma_\mu\psi)(\bar{\psi}\gamma^\mu\psi)]^2\end{aligned}$$

$$-\frac{1}{2}\delta_S\partial_\nu(\bar\psi\psi)\partial^\nu(\bar\psi\psi)-\frac{1}{2}\delta_V\partial_\nu(\bar\psi\gamma_\mu\psi)\partial^\nu(\bar\psi\gamma^\mu\psi)$$
$$-\frac{1}{2}\delta_{TV}\partial_\nu(\bar\psi\vec\tau\gamma_\mu\psi)\cdot\partial^\nu(\bar\psi\vec\tau\gamma^\mu\psi)$$
$$-\frac{1}{4}F^{\mu\nu}F_{\mu\nu}-e\bar\psi\gamma^\mu\frac{1-\tau_3}{2}\psi A_\mu, \quad (1)$$

which includes the free nucleon term, the four-fermion point-coupling terms, the higher-order terms which are responsible for the effects of medium dependence, the gradient terms which are included to simulate the effects of finite range, and the electromagnetic interaction terms. The Dirac spinor field of the nucleon is denoted by ψ, and the nucleon mass is m. α, β, γ, and δ with subscripts S (scalar), V (vector), and TV (isovector) are coupling constants (adjustable parameters) in which α refers to the four-fermion term, β and γ respectively to the third- and fourth-order terms, and δ to the derivative couplings.

Following the prescription in Ref. [18] where the BCS limit of finite-temperature Hartree-Fock Bogoliubov equations is derived, we obtain the finite-temperature CDFT+BCS equation. The finite-temperature Dirac equation for single nucleons reads

$$[\gamma_\mu(i\partial^\mu - V^\mu) - (m+S)]\psi_k = 0, \quad (2)$$

where m is the nucleon mass. $\psi_k(\boldsymbol{r})$ denotes the Dirac spinor field of a nucleon. The scalar $S(\boldsymbol{r})$ and vector $V^\mu(\boldsymbol{r})$ potentials are determined by the isoscalar density ρ_S, isoscalar current j_V^μ, and isovector current $\vec j_{TV}^\mu$. The density and currents are represented by

$$\rho_S(\boldsymbol{r}) = \sum_k \bar\psi_k(\boldsymbol{r})\psi_k(\boldsymbol{r})\big[v_k^2(1-2f_k)+f_k\big], \quad (3)$$

$$j_V^\mu(\boldsymbol{r}) = \sum_k \bar\psi_k(\boldsymbol{r})\gamma^\mu\psi_k(\boldsymbol{r})\big[v_k^2(1-2f_k)+f_k\big], \quad (4)$$

$$\vec j_{TV}^\mu(\boldsymbol{r}) = \sum_k \bar\psi_k(\boldsymbol{r})\vec\tau\gamma^\mu\psi_k(\boldsymbol{r})\big[v_k^2(1-2f_k)+f_k\big], \quad (5)$$

where the thermal occupation probability of quasiparticle states f_k is directly related to the temperature T by $f_k = 1/(1+e^{E_k/k_BT})$. E_k is the quasiparticle energy for the single-particle (s.p.) state k. A smooth energy-dependent cutoff weight g_k having the form of $\{1+\exp[(\epsilon_k-\lambda_q-E_c)/(E_c/10)]\}^{-1}$ is introduced to simulate the effect of finite range. The cutoff parameter E_c is further determined by an approximate condition $\sum_k 2g_k = N_q + 1.65N_q^{2/3}$ related to the particle number N_q [42]. Consequently, the quasiparticle energy reads $E_k = [(\epsilon_k-\lambda_q)^2+(g_k\Delta_k)^2]^{\frac{1}{2}}$, where λ_q is the Fermi level. In Eqs. (3)–(5), the BCS occupation probabilities v_k^2 and associated $u_k^2 = 1-v_k^2$ are obtained by

$$v_k^2 = \frac{1}{2}\left(1-\frac{\epsilon_k-\lambda_q}{E_k}\right), \quad (6)$$

$$u_k^2 = \frac{1}{2}\left(1+\frac{\epsilon_k-\lambda_q}{E_k}\right). \quad (7)$$

Δ_k is the pairing gap parameter, which satisfies the gap equation at finite temperature:

$$\Delta_k = -\frac{1}{2}\sum_{k'>0} V^{pp}_{k\bar k k'\bar k'}\frac{\Delta_{k'}}{E_{k'}}(1-2f_{k'}). \quad (8)$$

The particle number N_q is restricted by $N_q = 2\sum_{k>0}[v_k^2(1-2f_k)+f_k]$.

Here we take the δ pairing force $V(\boldsymbol{r}) = V_q\delta(\boldsymbol{r})$, where V_q is the pairing strength parameter for neutrons or protons. A smooth energy-dependent cutoff weight is introduced to simulate the effect of finite range in the evaluation of local pair density.

The internal binding energies E at deformation (β_2,β_3) are obtained by applying constraints on the quadrupole moment as well as the octupole moment. The free energy is evaluated by $F = E - TS$ where S is the entropy. The specific heat C_v is defined as $\partial E^*/\partial T$ where $E^*(T) = E(T) - E(T=0)$ is the internal excitation energy, and $E(T)$ is the internal binding energy for the global minimum state in the free energy surface at certain temperature T. Further details can be found in Ref. [39].

III. RESULTS AND DISCUSSION

The point-coupling density functional parameter set PC-PK1 is used in our calculation due to its success in the description of finite nuclei for both ground state and excited states [43]. The pairing correlations are taken into account by the BCS method with a δ pairing force. The value of the pairing strength V_q is taken from Refs. [44,45], that is, −333.9 (−397.0) MeV fm^3 for neutrons (protons). Such strengths are determined to reproduce the corresponding pairing gap of the spherical configuration of ^{300}Fm, calculated using the relativistic Hartree-Bogoliubov (RHB) model with the finite-size separable pairing force [44]. A set of axial harmonic oscillator basis functions with 20 major shells is used. Considering that the effects of the vapor phase become important when $T \geqslant 4.0$ MeV in the DHB calculations [37], we limit the temperature range to 0–4.0 MeV in our study.

First, we investigate the properties of ^{292}Cm, where the newly predicted mass region with octupole correlation is centered [41,46]. The free energies in the (β_2, β_3) plane at typical temperatures 0, 0.5, 0.8, 1.0, 1.2, and 1.6 MeV for ^{292}Cm are plotted in Fig. 1. The free energy surface at zero temperature in Fig. 1(a) reproduces Fig. 3(d) in Ref. [45] with the same parameter set and pairing strengths, as the free energy at zero temperature equals the binding energy. The calculated ground-state deformation ($\beta_2 = 0.177$, $\beta_3 = 0.166$) is close to other calculations with the parameter sets DD-PC1 ($\beta_2 = 0.150$, $\beta_3 = 0.137$) and NL3* ($\beta_2 = 0.155$, $\beta_3 = 0.136$) [46]. The quadrupole-deformed saddle point is about 1.8 MeV higher than the ground state. The free energy surfaces barely change in Figs. 1(a) and 1(b) for temperatures up to 0.5 MeV. In the temperature range $0.5 \leqslant T \leqslant 1.0$ MeV, the energy surfaces change dramatically. The energy difference between the saddle point and the global minimum quickly drops with slight changes of their deformations for $0.5 \leqslant T \leqslant 0.8$ MeV. At the same time, the energy difference between the global

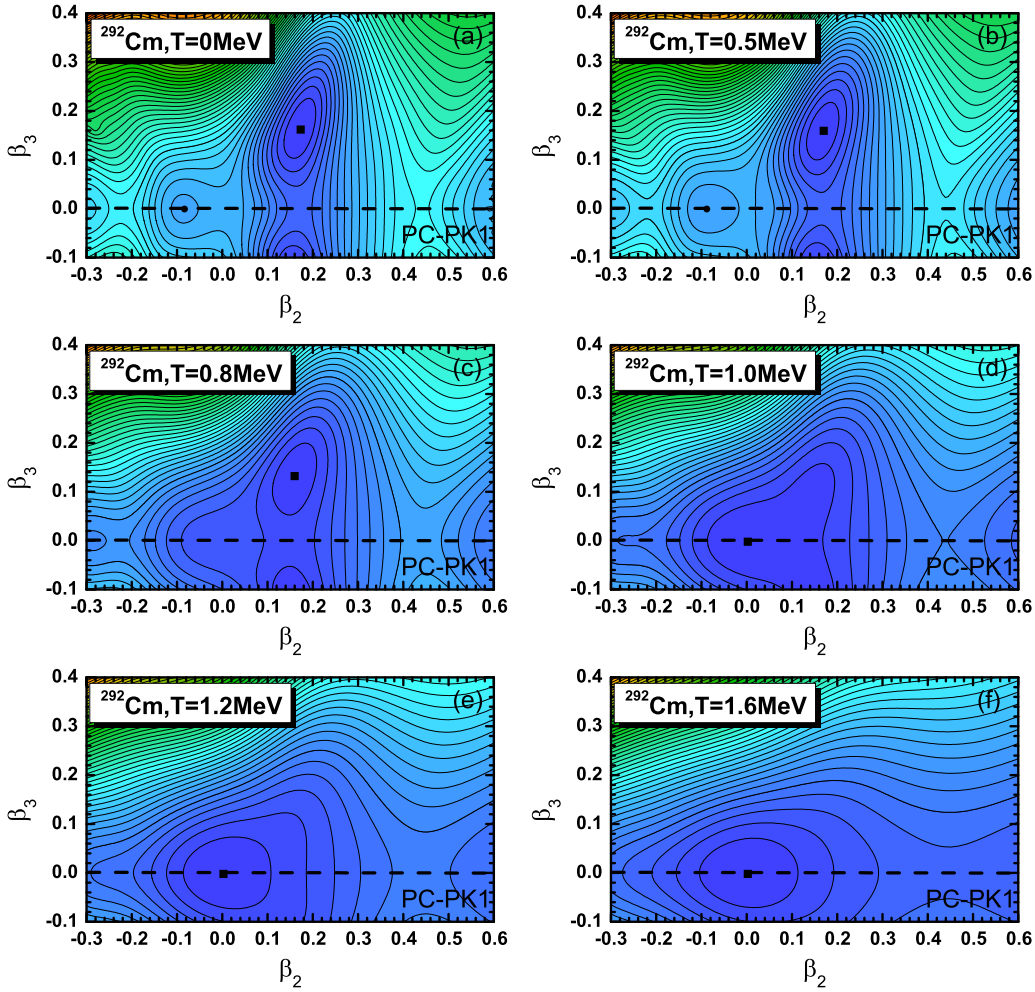

FIG. 1. The free energy surfaces in the (β_2, β_3) plane at temperature (a) $T = 0$, (b) $T = 0.5$, (c) $T = 0.8$, (d) $T = 1.0$, (e) $T = 1.2$(e), and (f) $T = 1.6$ MeV for ^{292}Cm obtained by the finite-temperature CDFT+BCS calculations using the PC-PK1 energy density functional. The global minima are indicated by the solid squares. The energy separation between contour lines is 0.5 MeV.

minimum and the spherical state also drops quickly, i.e., from 4.5 MeV at $T = 0.5$ MeV to 1.1 MeV at $T = 0.8$ MeV. At temperature 1.0 MeV in Fig. 1(d), the nucleus experiences a shape phase transition from quadrupole-octupole-deformed to spherical shape. When the temperature continues rising in Figs. 1(e) and 1(f), the global minimum remains at the spherical state while the soft area shrinks, especially in the β_3 direction. Such a shape evolution is similar to the evolution of ^{224}Ra [39], except that two shape transitions can be found for ^{224}Ra, namely, one from quadrupole-octupole-deformed shape to quadrupole-deformed shape at temperature 0.9 MeV, and the other from quadrupole-deformed shape to spherical shape at temperature 1.0 MeV. This could be related to the fact that the quadrupole deformation and octupole deformation of the ground state for ^{292}Cm are very close ($\beta_2 = 0.177, \beta_3 = 0.166$) while those for ^{224}Ra are separated ($\beta_2 = 0.184, \beta_3 = 0.133$). The possible relation between the shape transition temperatures and the ground-state deformations are analyzed later.

At zero temperature, the equilibrium shape tends to be deformed since it has lower values of the s.p. level density [3]. The s.p. levels of neutrons and protons of ^{292}Cm at zero temperature are plotted in Fig. 2. Two noticeable gaps or low level density areas at $N = 196$ and $Z = 96$ can be found around the ground state ($\beta_2 = 0.177$, $\beta_3 = 0.166$) in the right part of Fig. 2, which are responsible for the formation of octupole ground state.

In the axially deformed CDFT model, the s.p. levels are decomposed into various components of the harmonic basis with the same quantum number Ω (projection of the total angular momentum onto the symmetry axis), and further labeled by the primary one. As the level components and their decomposition contributions vary with the deformations, the primary component (i.e., the level label) may change at certain deformations. Taking the level $\nu 1/2[750]$ near the Fermi surface at the ground state as an example, its primary component changes to $1/2[770]$, and then to $1/2[860]$ when β_3 decreases from 0.166 towards the purely quadrupole-deformed state. Since the octupole correlation couples the orbitals with $\Omega[N, n_z, m_l]$ and $\Omega[N+1, n_z \pm 3, m_l]$ [47], it is interesting to investigate how the octupole correlation plays a role in ^{292}Cm by examining the detailed components of its s.p. levels, at quadrupole-octupole-deformed (octupole deformed for short)

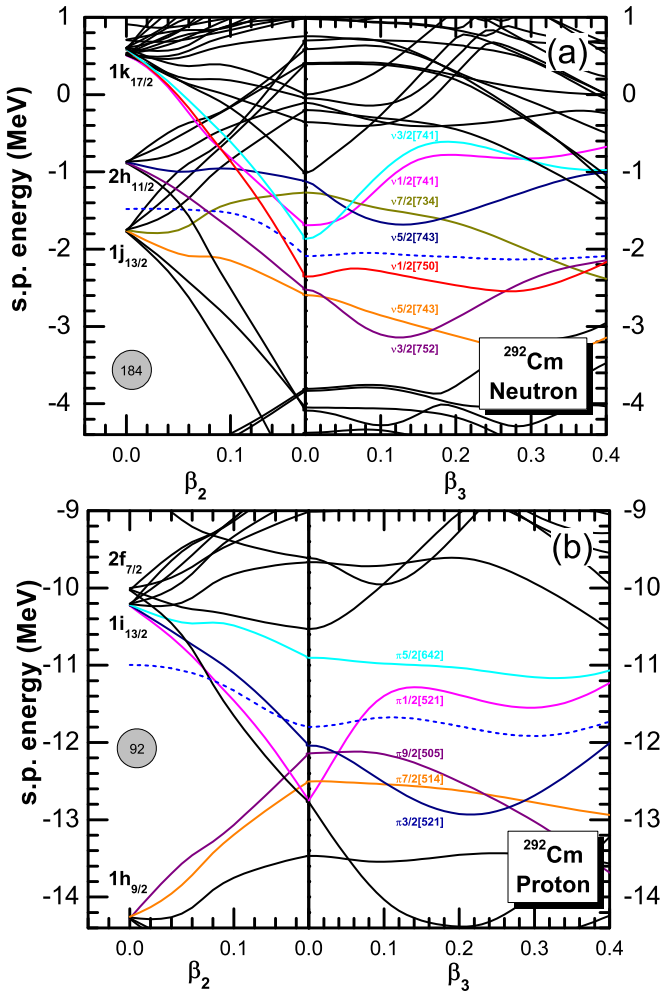

FIG. 2. (a) Neutron and (b) proton single-particle levels as a function of deformation for the nucleus ^{292}Cm, obtained by the constrained CDFT+BCS calculations using the PC-PK1 energy density functional. The dash-dotted lines denote the corresponding Fermi surfaces. In the left portion, the quadrupole deformation β_2 increases from zero to 0.177 without octupole deformation, while in the right portion, the octupole deformation β_3 increase from zero to 0.4 with $\beta_2 = 0.177$. The single-particle level $\nu 1/2[750]$ denoted in red is analyzed in Table I.

state or purely quadrupole-deformed state, before and after the shape transition temperature. The components of the s.p. level labeled as $\nu 1/2[750]$ at the ground state and at the quadrupole-deformed state (its label changes into 1/2[860] as described above) are compared side by side in Table I. To save space, the left four columns are for the octupole-deformed state while the right two columns are for the quadrupole-deformed state. Unfortunately, the octupole pairing partner of the first leading component 1/2[750] cannot be found in the components contributing no less than 1%. For the second leading component 1/2[741], two octupole pairing partners can be found, namely, 1/2[871] and 1/2[611]. Together they compose two driving pairs 1/2[741] − 1/2[871] and 1/2[741] − 1/2[611], which satisfies the rule that the quantum number N differs by 1 and n_z differs by 3. Similarly, for the third leading

TABLE I. The components of single-particle level $\nu 1/2[750]$ [denoted in red in Fig. 2(a)] at the ground state (g.s.) with $(\beta_2,\beta_3) = (0.172,0.166)$ and quadrupole state (q.s.) with $(\beta_2,\beta_3) = (0.172,0)$ at zero temperature in ^{292}Cm, obtained by the constrained CDFT+BCS calculations using the PC-PK1 energy density functional. Only the components contributing no less than 1% are listed. The summed octupole-component contribution is listed at the bottom.

g.s. at $T = 0$ MeV				q.s. at $T = 0$ MeV	
1/2[750]	17.1%	1/2[741]	14.6%	1/2[860]	24.1%
1/2[770]	8.9%	1/2[871]	3.7%	1/2[851]	17.5%
1/2[840]	5.3%	1/2[611]	1.6%	1/2[840]	13.1%
1/2[640]	3.9%	1/2[721]	7.7%	1/2[871]	11.9%
1/2[970]	2.9%	1/2[851]	3.8%	1/2[880]	9.2%
1/2[10,10,0]	1.7%	1/2[981]	2.3%	1/2[831]	4.5%
1/2[990]	6.3%	1/2[530]	1.5%	1/2[660]	3.4%
1/2[860]	2.4%	1/2[660]	1.4%	1/2[651]	3.0%
1/2[11,11,0]	1.1%	1/2[761]	1.1%	1/2[10,10,0]	1.7%
1/2[710]	1.0%			1/2[640]	1.5%
				1/2[820]	1.3%
Sum			68.2%		0%

component, there are four driving pairs 1/2[770] − 1/2[840], 1/2[770] − 1/2[640], 1/2[840] − 1/2[970], and 1/2[970] − 1/2[10,10,0]; for the fourth component, there are two pairs 1/2[721] − 1/2[851] and 1/2[851] − 1/2[981]; and for the remaining components, there are two pairs 1/2[990] − 1/2[860] and 1/2[530] − 1/2[660]. Finally, all components composing octupole driving pairs contribute an outstanding portion of 68.2% by counting only once. For the quadrupole-deformed state, this level only has the components with even N numbers, making the octupole pairs apparently absent.

For completeness, the contributions from octupole driving components for other s.p. levels near the Fermi surfaces for octupole-deformed ground state and quadrupole-deformed state are tabulated in the left part of Table II. It is clear that, for the octupole-deformed ground state, the octupole driving components contribute a large portion to all the neutron s.p. levels and some proton s.p. levels near the Fermi surfaces. On the contrary, the octupole driving components contribute nothing to the s.p. levels for the quadrupole-deformed state at zero temperature. In the right part of Table II, the contribution for such s.p. levels before and at the shape transition temperature 1.0 MeV are listed. The situation for the global minimum state at $T = 0.8$ MeV is very similar to the global minimum state at $T = 0$ MeV, manifested by the existence of big octupole deformation at $T = 0.8$ MeV. After the shape transition, the contributions of octupole driving components become zero, and consequently the octupole deformation disappears as well at $T = 1.0$ MeV. Based on this table, the contribution coming from the octupole driving pairs for s.p. levels near the Fermi surfaces provides a good manifestation of the octupole correlation in the axially deformed CDFT model.

Furthermore, we discuss the deformations, and the pairing gaps of the global minimum as functions of temperature for even-even $^{286-304}$Cm isotopes. Figure 3 displays the deformations β_2, β_3, and β_4 as functions of temperature for even-even $^{286-304}$Cm. At zero temperature, the values of β_2, β_3

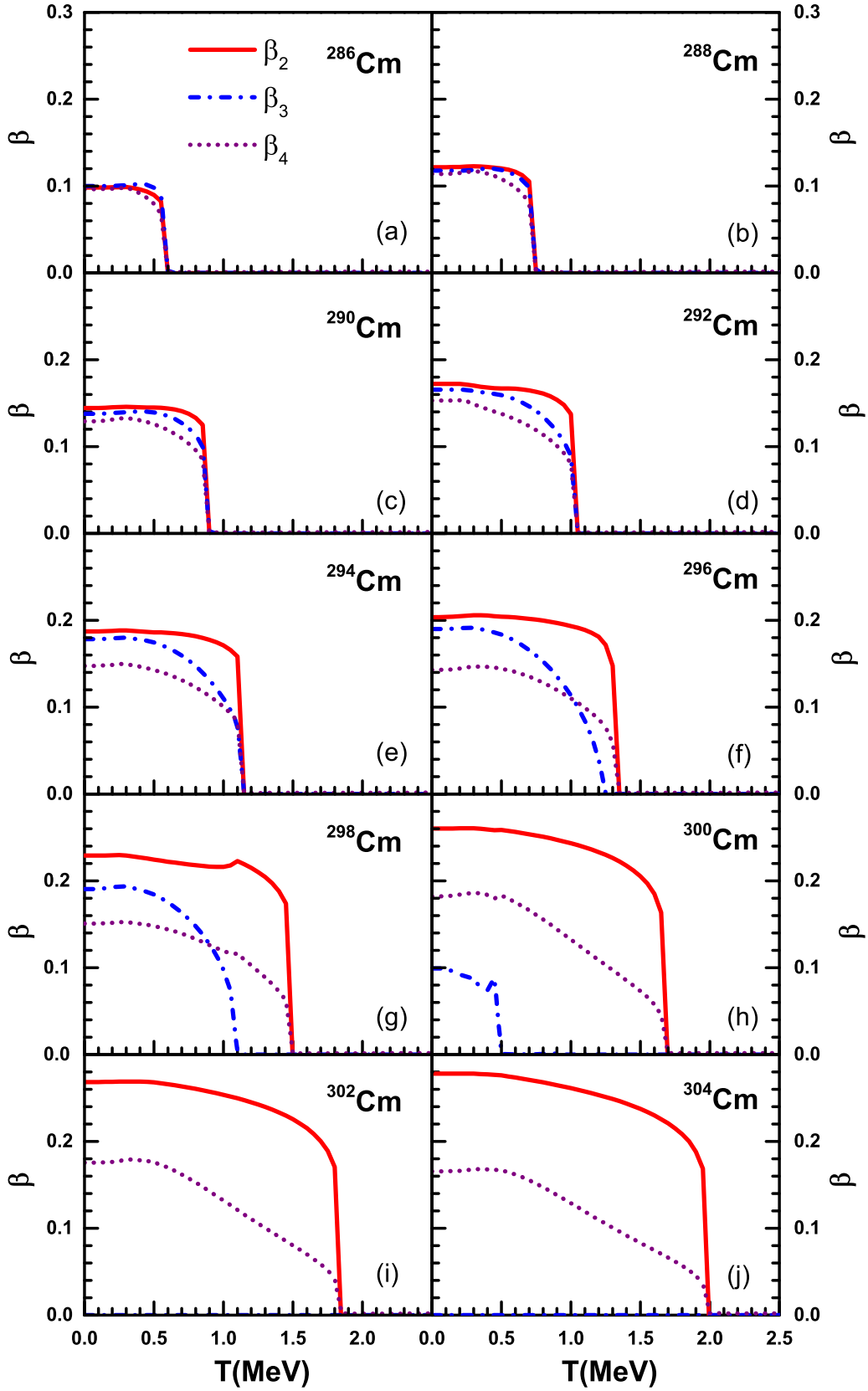

FIG. 3. The global minimum deformations β_2, β_3, β_4 as functions of temperature (in MeV) for even-even $^{286-304}$Cm (a-j), obtained by the finite-temperature CDFT+BCS calculations using PC-PK1 energy density functional.

TABLE II. Summed contribution from the octupole driving pairs $\Omega[N,n_z,m_l]$ and $\Omega[N+1,n_z\pm3,m_l]$ for single-particle levels near Fermi surfaces at the ground state (g.s.) with $(\beta_2,\beta_3)=(0.172,0.166)$ and quadrupole state (q.s.) with $(\beta_2,\beta_3)=(0.172,0)$ at $T=0$ MeV, as well as the global minimum state (g.m.) with $(\beta_2,\beta_3)=(0.161,0.135)$ at $T=0.8$ MeV and the global minimum state (g.m.) with $(\beta_2,\beta_3)=(0,0)$ at $T=1$ MeV in ^{292}Cm, obtained by the constrained CDFT+BCS calculations using PC-PK1 energy density functional. See Table I for summation detail.

Level	g.s. at $T=0$ MeV	q.s. at $T=0$ MeV	g.m. at $T=0.8$ MeV	g.m. at $T=1$ MeV
$\nu3/2[752]$	85.9%	0%	52.0%	0%
$\nu5/2[743]$	69.6%	0%	67.9%	0%
$\nu1/2[750]$	68.2%	0%	69.8%	0%
$\nu5/2[743]$	46.9%	0%	53.3%	0%
$\nu7/2[734]$	36.3%	0%	22.8%	0%
$\nu1/2[741]$	62.7%	0%	66.1%	0%
$\nu3/2[741]$	70.9%	0%	89.7%	0%
$\pi3/2[521]$	69.8%	0%	70.2%	0%
$\pi7/2[514]$	0%	0%	0%	0%
$\pi9/2[505]$	0%	0%	0%	0%
$\pi1/2[521]$	70.7%	0%	71.3%	0%
$\pi5/2[642]$	51.6%	0%	51.9%	0%

for even-even $^{286-296}$Cm are nearly identical. For ^{298,300}Cm, the octupole deformation β_3 becomes smaller, and finally for ^{302,304}Cm it disappears. Such results at zero temperature are consistent with calculations of parameter sets DD-PC1 [46] and NL3* [46]. For example, the ground-state deformation (β_2,β_3) for ^{296}Cm reads (0.204,0.190) for PC-PK1, (0.190,0.164) for DD-PC1, and (0.189,0.154) for NL3*. The increasing quadrupole deformation for even-even $^{286-304}$Cm ground states can be associated with the fact that the neutron number is departing from 184, where shell closure is predicted in the CDFT calculations, toward the middle of a new shell closure. For each isotope, when the temperature rises, the global minimum deformations evolve with the temperature similarly, where they change slowly for temperatures far below the transition temperature and then quickly drop to zero approaching the transition temperature. The quadrupole and octupole transition temperatures for ^{298,300}Cm are separated, similar to the case of ^{224}Ra and even-even $^{144-154}$Ba discussed in Ref. [39]. The hexadecapole deformation β_4 behaves like β_2 and β_3 for $^{286-296}$Cm, while it drops little at the octupole transition temperature and vanishes at the quadrupole transition temperature for ^{298,300}Cm. The quadrupole and octupole shape transition temperatures T_2 and T_3 increase with the corresponding deformations as well. We analyze in more detail their relations in Figs. 5 and 6.

The pairing gaps for neutrons and protons, Δ_n and Δ_p, as functions of temperature are displayed in Fig. 4. Both neutron and proton pairing correlations exist for even-even $^{286-304}$Cm at low temperatures. The neutron pairing gaps are $0.4\sim0.5$ MeV while the proton pairing gaps are $0.7\sim0.9$ MeV. All critical temperatures for pairing phase transition basically follow the rule $T_{n,p}=0.6\Delta_{n,p}(0)$, where $T_{n,p}$ is the neutron or proton pairing phase transition temperature and $\Delta_{n,p}(0)$ is the neutron or proton pairing gap at zero temperature. This rule was discovered for spherical nuclei in Refs. [17,19,33].

Prompted by the simple relation between the pairing transition temperatures and the pairing gaps at zero temperature, we study the possible relation between the shape transition temperatures and the deformations at zero temperature. In Fig. 5, the critical shape transition temperatures T_2 (T_3) versus the ground-state quadrupole and octupole deformations β_2 (β_3) (0) for even-even $^{284-304}$Cm are plotted. It turns out that a good proportional relation between the critical temperature and deformation is found, which is $T_{2,3}=6.6\beta_{2,3}(0)$ for both quadrupole and octupole shape transitions. This ratio is obtained based on our microscopic calculations from the covariant density functional. From Ref. [2], it indicates a larger ratio, where the difference may come from the different functionals or different ways to treat pairing correlations. So more studies based on different microscopic theory frameworks are encouraged. In a previous study, the ratio was estimated to be $40A^{-1/3}$ [48], which is consistent with our results. Since the nuclei we considered here are heavy nuclei, the dependence on mass number is unnoticeable. However, further systematic investigation will be done in the future.

For even-even $^{284-304}$Cm, the shape transition temperatures $T_{2,3}$ and the quadrupole and octupole deformations at zero temperature $\beta_{2,3}(0)$ as well as $6.6\beta_{2,3}(0)$ as functions of the neutron numbers are plotted in Figs. 6(a) and 6(b), respectively; the pairing transition temperatures for neutrons and protons $T_{n,p}$, the pairing gap at zero temperature for neutrons and protons $\Delta_{n,p}(0)$, as well as $0.6\Delta_{n,p}(0)$, are plotted in Figs. 6(c) and 6(d). Similar to Ref. [24], the quadrupole deformation at zero temperature, $\beta_2(0)$, monotonously increases starting from ^{286}Cm with rising neutron numbers since it starts from the shell closure and is reaching the middle of the shell. The quadrupole shape transition temperature T_2 has the same behavior as $\beta_2(0)$ in Fig. 6(a). In between purely quadrupole-deformed ^{284}Cm and ^{302}Cm, the octupole deformation $\beta_3(0)$ first slowly increases and quickly decreases after nucleus ^{298}Cm. Such a pattern should also hold for $\beta_2(0)$ if more neutron-rich isotopes are included. From Figs. 6(a) and 6(b) we can see for both quadrupole and octupole shape transitions that the critical temperature follows $T_c=6.6\beta(0)$ very well. Similarly, in Figs. 6(c) and 6(d), the critical temperature for pairing transition also follows $T_c=0.6\Delta(0)$.

Finally, the specific heat C_v as a function of temperature for even-even $^{286-304}$Cm is plotted in Fig. 7. The specific heat is the derivative of the relative excitation energy E^*, and the discontinuities in this quantity are customarily interpreted as a signature of phase transitions. There are three discontinuities for even-even $^{286-304}$Cm except ^{298}Cm, indicating neutron pairing transition, proton pairing transition, and shape transition from octupole-quadrupole-deformed shape to spherical shape. Since the quadrupole and octupole ground-state deformations for ^{298,300}Cm are separated, two separated shape transitions occur, namely, one from octupole-quadrupole-deformed shape to quadrupole-deformed shape and the other from quadrupole-deformed shape to spherical shape. So for ^{298}Cm, there are four transitions: pairing transitions at $T=0.3$ and 0.5 MeV,

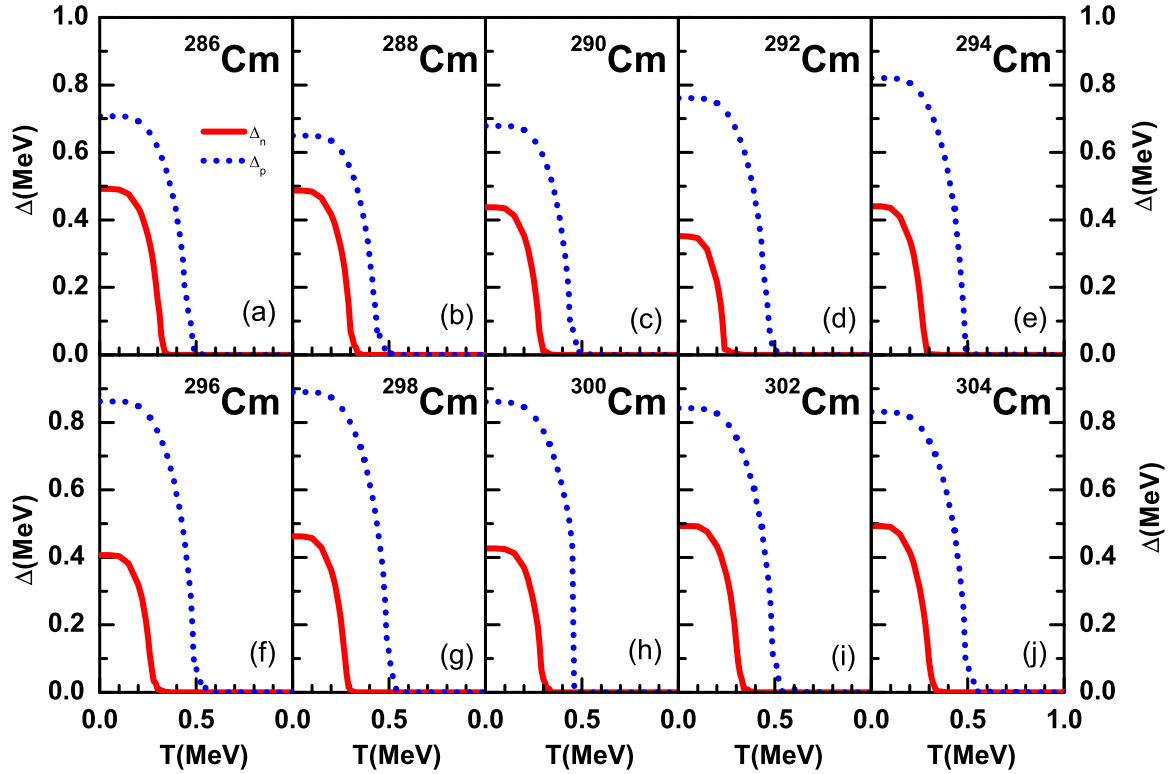

FIG. 4. The pairing gaps for neutrons and protons, Δ_n and Δ_p (in MeV), as functions of temperature (in MeV) for (a)–(j) even-even $^{286-304}$Cm, obtained by the finite-temperature CDFT+BCS calculations using the PC-PK1 energy density functional.

octupole shape transition at $T = 1.1$ MeV, and quadrupole shape transitions at $T = 1.5$ MeV. For ^{300}Cm, the proton pairing transition coincides with the octupole shape transition at $T = 0.5$ MeV, making three discontinuities in C_v. With increasing neutron numbers, the discontinuities caused by pairing transitions almost stay the same at $T = 0.3$ and 0.5 MeV, while the discontinuity caused by shape transitions move to high temperatures monotonously. All the discontinuities in the

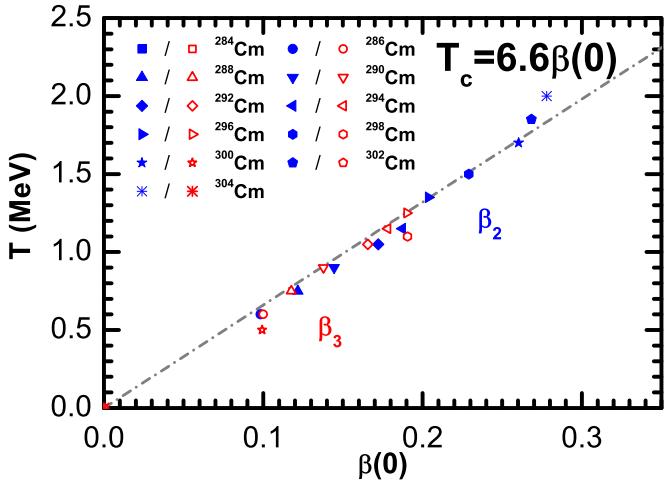

FIG. 5. The quadrupole (octupole) transition temperatures T_2 (T_3) versus the corresponding ground-state deformations β_2 (β_3) (0) for even-even $^{284-304}$Cm obtained by the constrained CDFT+BCS calculations using the PC-PK1 energy density functional. The dash-dotted line indicates the proportional relation $T_c = 6.6\beta(0)$. The solid and open symbols refer to quadrupole and octupole deformations correspondingly.

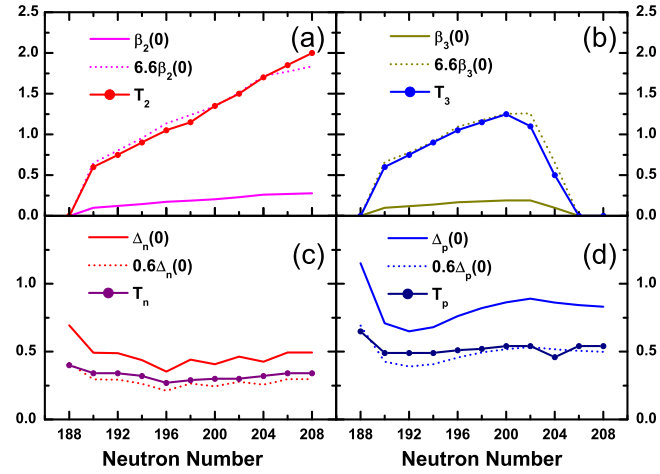

FIG. 6. The ground-state (a) quadrupole and (b) octupole deformations, $\beta_2(0)$ and $\beta_3(0)$, as well as $6.6\beta_2(0)$ and $6.6\beta_3(0)$, and their corresponding shape transition temperatures T_2 and T_3, and the ground-state pairing gaps for (c) neutrons and (d) protons, $\Delta_n(0)$ and $\Delta_p(0)$, as well as $0.6\Delta_n(0)$ and $0.6\Delta_p(0)$, and their corresponding pairing transition temperatures T_n and T_p, as functions of neutron number for even-even $^{284-304}$Cm, obtained by the constrained CDFT+BCS calculations using the PC-PK1 energy density functional. The transition temperatures and pairing gaps are in MeV.

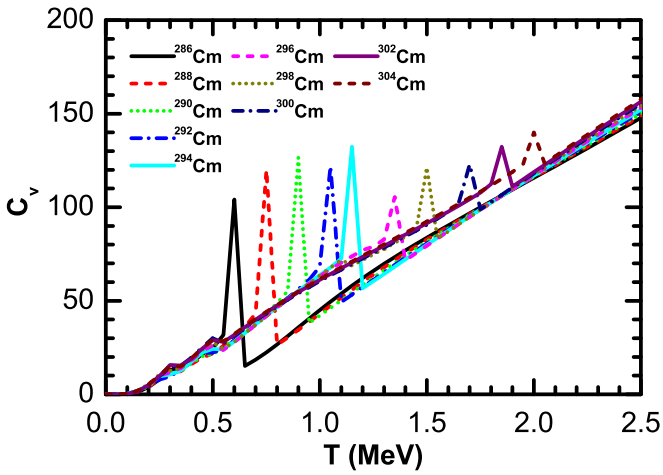

FIG. 7. The specific heat C_v as a function of temperature (in MeV) for even-even $^{286-304}$Cm, obtained by the finite-temperature CDFT+BCS calculations using the PC-PK1 energy density functional.

specific heat will be more moderate if the quantum fluctuation is further considered.

IV. SUMMARY

In summary, the shape evolutions of even-even $^{286-304}$Cm with temperature are studied using the finite-temperature axially deformed CDFT+BCS theory. As a typical example in these isotopes, we studied in detail the free energy surface, the Nilsson single-particle levels, and the components of s.p. levels near the Fermi level in ^{292}Cm. Through this study, the formation of octupole equilibrium is understood by the contribution coming from the octupole driving pairs with $\Omega[N,n_z,m_l]$ and $\Omega[N+1,n_z\pm 3,m_l]$ for single-particle levels near the Fermi surfaces as it provides a good manifestation of the octupole correlation in the axially deformed CDFT model. Furthermore, the deformations, and the pairing gaps of the global minimum together with the specific heat as functions of the temperature for even-even $^{286-304}$Cm isotopes are discussed. A simple relation between the shape transition temperatures and the deformations at zero temperature $T_c = 6.6\beta(0)$ is found valid for both octupole shape transition and quadrupole shape transition for the isotopes considered.

ACKNOWLEDGMENTS

This work was supported in part by National Natural Science Foundation of China under Grants No. 11105042, No. 11305161, and No. 11505157, China Scholarship Council, and Physics Research and Development Program of Zhengzhou University under Grant No. 32410017. The theoretical calculation was carried out by the nuclear data storage system in Zhengzhou University. Work at the Molecular Foundry, Lawrence Berkeley National Laboratory, was supported by the Office of Science, Office of Basic Energy Sciences, of the U.S. Department of Energy under Contract No. DE-AC02-05CH11231. W.Z. visit in Lawrence Berkeley National Laboratory is supported by China Scholarship Council.

[1] J. L. Egido and P. Ring, J. Phys. G **19**, 1 (1993).
[2] J. L. Egido, L. M. Robledo, and V. Martin, Phys. Rev. Lett. **85**, 26 (2000).
[3] S. Levit and Y. Alhassid, Nucl. Phys. A **413**, 439 (1984).
[4] P. Ring, L. M. Robledo, J. L. Egido, and M. Faber, Nucl. Phys. A **419**, 261 (1984).
[5] A. Schiller and M. Thoennessen, At. Data Nucl. Data Tables **93**, 549 (2007).
[6] Y. F. Niu, N. Paar, D. Vretenar, and J. Meng, Phys. Lett. B **681**, 315 (2009).
[7] D. R. Chakrabarty, N. Dinh Dang, and V. M. Datar, Eur. Phys. J. A **52**, 143 (2016).
[8] E. Yuksel, G. Colo, E. Khan, Y. F. Niu, and K. Bozkurt, Phys. Rev. C **96**, 024303 (2017).
[9] V. Martin, J. L. Egido, and L. M. Robledo, Phys. Rev. C **68**, 034327 (2003).
[10] Y. Alhassid and J. Zingman, Phys. Rev. C **30**, 684 (1984).
[11] R. Rossignoli and P. Ring, Ann. Phys. **235**, 350 (1994).
[12] G. H. Lang, C. W. Johnson, S. E. Koonin, and W. E. Ormand, Phys. Rev. C **48**, 1518 (1993).
[13] N. D. Dang, P. Ring, and R. Rossignoli, Phys. Rev. C **47**, 606 (1993).
[14] N. D. Dang, Phys. Rev. C **76**, 064320 (2007).
[15] D. Gambacurta, D. Lacroix, and N. Sandulescu, Phys. Rev. C **88**, 034324 (2013).
[16] L. Liu, Z. H. Zhang, and P. W. Zhao, Phys. Rev. C **92**, 044304 (2015).
[17] M. Sano and S. Yamasaki, Prog. Theor. Phys. **29**, 397 (1963).
[18] A. L. Goodman, Nucl. Phys. A **352**, 30 (1981).
[19] Y. F. Niu, Z. M. Niu, N. Paar, D. Vretenar, G. H. Wang, J. S. Bai, and J. Meng, Phys. Rev. C **88**, 034308 (2013).
[20] Y. F. Niu, N. Paar, D. Vretenar, and J. Meng, Phys. Rev. C **83**, 045807 (2011).
[21] C.-W. Ma, F. Niu, C.-Y. Qiao, Y. F. Niu, and T.-Z. Yan, Phys. Rev. C **94**, 024615 (2016).
[22] C.-W. Ma, C.-Y. Qiao, T.-T. Ding, F. Niu, Y.-D. Song, and Y. F. Niu, Commun. Theor. Phys. **66**, 122 (2016).
[23] Y. Alhassid, S. Levit, and J. Zingman, Phys. Rev. Lett. **57**, 539 (1986).
[24] Y. Alhassid, J. M. Manoyan, and S. Levit, Phys. Rev. Lett. **63**, 31 (1989).
[25] A. L. Goodman, Phys. Rev. C **34**, 1942 (1986).
[26] P. Ring, Prog. Part. Nucl. Phys. **37**, 193 (1996).
[27] S.-G. Zhou, J. Meng, and P. Ring, Phys. Rev. Lett. **91**, 262501 (2003).
[28] D. Vretenar, A. V. Afanasjev, G. A. Lalazissis, and P. Ring, Phys. Rep. **409**, 101 (2005).
[29] J. Meng, H. Toki, S.-G. Zhou, S. Q. Zhang, W. H. Long, and L. S. Geng, Prog. Part. Nucl. Phys. **57**, 470 (2006).

[30] J. Meng, J. Peng, S. Q. Zhang, and S.-G. Zhou, Phys. Rev. C **73**, 037303 (2006).
[31] H. Z. Liang, J. Meng, and S.-G. Zhou, Phys. Rep. **570**, 1 (2015).
[32] *Relativistic Density Functional for Nuclear Structure*, edited by J. Meng (World Scientific, Singapore, 2016).
[33] J. J. Li, J. Margueron, W. H. Long, and N. Van Giai, Phys. Rev. C **92**, 014302 (2015).
[34] B. K. Agrawal, T. Sil, J. N. De, and S. K. Samaddar, Phys. Rev. C **62**, 044307 (2000).
[35] B. K. Agrawal, T. Sil, S. K. Samaddar, and J. N. De, Phys. Rev. C **63**, 024002 (2001).
[36] P. Bonche, S. Levit, and D. Vautherin, Nucl. Phys. A **427**, 278 (1984); **436**, 265 (1985).
[37] R. Lisboa, M. Malheiro, and B. V. Carlson, Phys. Rev. C **93**, 024321 (2016).
[38] W. Zhang and Y. F. Niu, Chin. Phys. C **41**, 094102 (2017).
[39] W. Zhang and Y. F. Niu, Phys. Rev. C **96**, 054308 (2017).
[40] P. A. Butler and W. Nazarewicz, Rev. Mod. Phys. **68**, 349 (1996).
[41] S. E. Agbemava and A. V. Afanasjev, Phys. Rev. C **96**, 024301 (2017).
[42] M. Bender, K. Rutz, P.-G. Reinhard, and J. A. Maruhn, Eur. Phys. J. A **8**, 59 (2000).
[43] P. W. Zhao, Z. P. Li, J. M. Yao, and J. Meng, Phys. Rev. C **82**, 054319 (2010).
[44] T. Nikšić, D. Vretenar, and P. Ring, Comput. Phys. Commun. **185**, 1808 (2014).
[45] Z. Xu and Z. P. Li, Chin. Phys. C **41**, 124107 (2017).
[46] S. E. Agbemava, A. V. Afanasjev, and P. Ring, Phys. Rev. C **93**, 044304 (2016).
[47] W. Nazarewicz, in *Nuclear Shapes and Nuclear Structure at Low Excitation Energies*, edited by M. Vergnes *et al.* (Plenum Press, New York, 1992), p. 258.
[48] S. Björnholm, A. Bohr, and B. Mottelson, in *Proceedings of the International Conference on the Physics and Chemistry of Fission* (IAEA, Vienna, 1974), Vol. 1, p. 367.